

Employing spatial information technologies to monitor biological control of saltcedar in West Texas

Reginald S. Fletcher*

USDA-ARS-Crop Production Systems Research Unit, Stoneville, MS, USA

(Received 21 August 2012; final version received 16 January 2013)

The saltcedar leaf beetle (*Diorhadha* spp.) has shown promise as a biocontrol agent for saltcedar (*Tamarix* spp.) invasions in the USA. In Texas, natural resource managers need assistance in monitoring biological control of invasive saltcedars. This study describes application of a medium-format, digital camera acquiring natural colour imagery and global positioning system (GPS) and geographic information system (GIS) technologies to check biological control of saltcedar in west Texas. On 8 July and 8 September 2011, natural colour airborne digital imagery was collected along a 155.8 km transect covering portions of Presidio and Brewster counties of Texas. The camera was tethered to a GPS receiver that geotagged each image and saved the coordinates to a key-hole marked up language file that was viewable on Google Earth. Saltcedar trees exhibiting severe feeding damage and those that were totally defoliated were easily identified in the imagery. The former appeared in orange to brown colour tones; the latter exhibited grey colour tones. Point distribution maps showing locations of saltcedar trees exhibiting feeding damage were developed from GPS information in the GIS. Coordinate points on the map were linked to the corresponding image, permitting the user to have quick access to view imagery. The results of this study show a practical method for monitoring biological control of saltcedar.

Keywords: remote sensing; saltcedar leaf beetle; geographic information system; global positioning system; Hasselblad

1. Introduction

Beginning in 1823, *Tamarix* spp., tree to shrub-like plants native to Eurasia, was introduced into the USA as ornamentals, for stream channel stabilization, and as wind-breaks (Brotherson & Winkel 1986; DiTomaso 1998). Eighteen species exists in the USA (Baum 1967; Crins 1989); several species have become invasive including, *T. ramosissima*, *T. chinensis*, *T. parviflora*, and their hybrids (Gaskin & Schaal 2002, 2003; USDA 2005).

Saltcedars are classified as phreatophytic and facultative holophytic plants. In the USA, the plants are not affected by fire, drought conditions, and inundation by water, are difficult to control with herbicides or bulldozing, and are not attacked by local

*Email: reginald.fletcher@ars.usda.gov

This project was funded by USDA-ARS; mention of trade names or commercial products in this publication is solely for the purpose of providing specific information and does not imply recommendation or endorsement by the USDA.

This work was authored as part of the Contributor's official duties as an Employee of the United States Government and is therefore a work of the United States Government. In accordance with 17 U.S.C. 105, no copyright protection is available for such works under U.S. Law.

insects, making it the ideal invasive weed in riparian systems. Baker (1974) indicated that saltcedar has nine out of 12 of the characteristics contributing to the success of a plant as an invasive weed. These plants use excessive amounts of water, lowering water tables and decreasing the ability of other plants to survive in riparian areas. Additionally, saltcedars are able to use saline water for growth, leading to excretion of excessive salts from special glands in the leaves. Eventually, these leaves fall to the ground, adding additional salts to surface soils and reducing the ability of non-salt-tolerant plants to grow in those areas. Fallen foliage is highly flammable, increasing the fire load. Over time, desertification and salinization of the watershed result in localized extinction of native trees and ultimately to complete dominance of the floodplain by mono-specific saltcedar thickets (DeLoach et al. 2000).

Mechanical and chemical management methods are not effective for controlling saltcedar. Also, these techniques are expensive, labour intensive and require frequent treatments. Furthermore, chemical control measures for saltcedar invasion have a negative impact on other plants within the immediate area. The shortcomings of mechanical and chemical methods have lead researchers to evaluate and promote biological control measures to contain saltcedar invasions.

Biological control efforts have focused on releasing and establishing the *Diorhadha* spp., commonly referred to as the saltcedar leaf beetle. Since 1994, four species (*D. carinulata*, *D. sublineata*, *D. elongate*, and *D. carinata*) have been introduced into the USA and have shown promise for controlling saltcedar invasions. It is important to point out that this biological method does not eradicate the infestation, but it does provide a means of slowing down the spread of saltcedar.

Once established, the saltcedar leaf beetle and larvae feed on the leaves of saltcedar trees until the trees are totally defoliated. Then the beetles move on to another location with saltcedar trees. The trees that were defoliated will re-leaf and then the cycle is repeated. The defoliation–re-leaf cycle begins in the spring and continues until the fall. Adult beetles overwinter in the soil until the next spring, at which time the cycle begins again.

Defoliation reduces the plant's ability to conduct photosynthesis. Re-leafing causes the plant to use excessive energy weakening it over time. The defoliation–re-leafing process will eventually kill the tree; however, death may not occur for many years. Natural resource managers are looking for efficient and cost-effective ways to monitor biological control of saltcedar.

Remote sensing may offer the best solution to this problem. Imagery captured from airborne or space-borne platforms provide a 'bird's eye view' of the area of interest, thus covering a large area in a single frame. Airborne imaging systems also give users the capability to acquire imagery at different altitudes, affording analysts the ability to change the spatial resolution of pixels based on altitude.

Normalized difference vegetation index (NDVI) imagery derived from satellite sensors has shown promise as a tool to monitor chemical and biological control of saltcedar. Nagihara and Hart (2007) employed sequential NDVI imagery created using Landsat Thematic Mapper (TM) 7 and the Advanced Spaceborne Thermal Emission and Reflection Radiometer (ASTER) to monitor chemical defoliation of saltcedar with herbicides along the lower Pecos River in the USA. Defoliation of saltcedar trees by the saltcedar leaf beetle was detected with temporal NDVI imagery produced with ASTER and Moderate Resolution Imaging Spectrometer (MODIS) data. Coarse spatial resolution of those satellites limit applications to dense stands of saltcedar and to large areas affected by saltcedar; in smaller areas, mixed pixels

becomes an issue (Nagihara & Hart 2007; Dennison et al. 2009). More research is needed on the application of high-resolution imagery for monitoring biological control of saltcedar.

High-resolution airborne remote-sensing systems and geographic information system (GIS) and global positioning systems (GPS) technologies have been integrated to develop distribution maps of aquatic and terrestrial weed infestations. Previous studies have focused on using aerial videography as the major means for image acquisition (Everitt et al. 1994, 1996, 1999, 2003, 2006). Everitt et al. (2007) used aerial colour photography subjected to computer classification to assess saltcedar beetle and larvae feeding damage to saltcedar trees. For that study, associated cover types were removed to obtain good classification accuracy. That technique would be tedious for large areas. In addition, the cost of processing the film is an additional expense. No information is available on using high-resolution true digital imagery, and GIS and GPS technologies to monitor biological control of saltcedar in a practical way. This study describes application of airborne natural colour digital imagery and GPS and GIS technologies to monitor biological control of saltcedar in west Texas.

2. Materials and methods

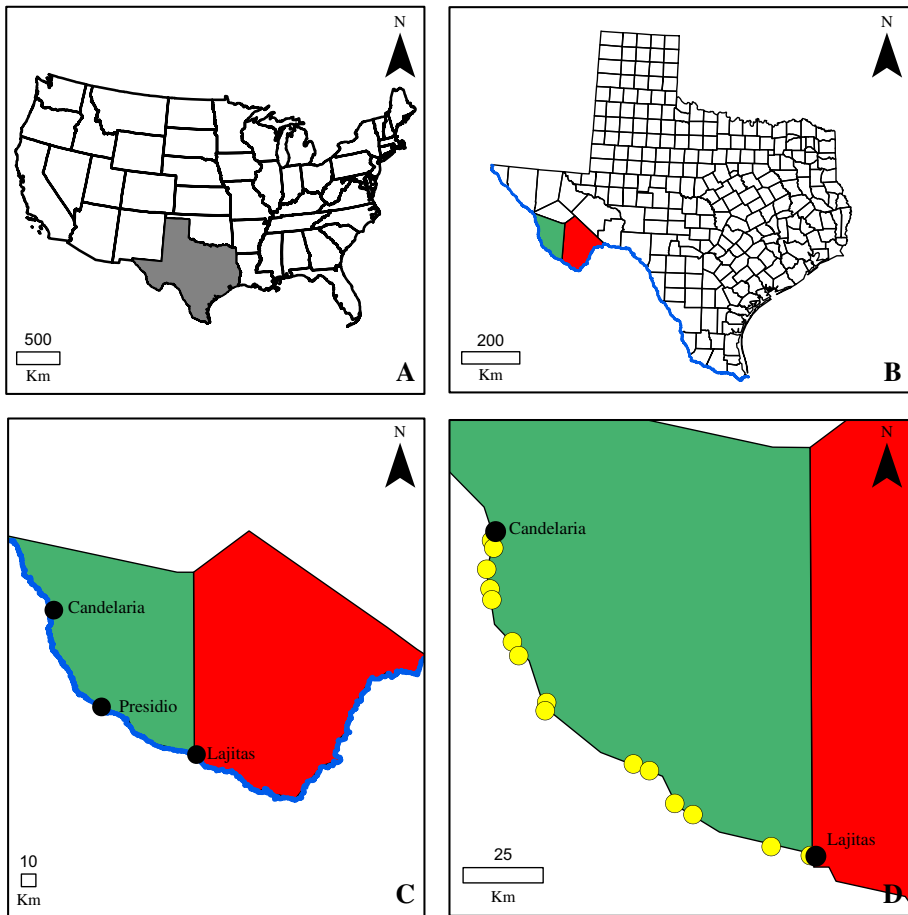
2.1. Study site

The study occurred along a 155.8 km transect (transect measure in road miles; Figure 1) within the Chihuahuan desert. It started approximately 1.6 km northwest of Candelaria, Texas and ended in Lajitas, Texas. The former and latter are cities within Presidio County and Brewster County, respectively. *Diorhadha* spp. have been released at 15 sites (Jack DeLoach and James Tracy; personal communication) along the transect (Table 1, Figure 1).

2.2. Camera system

A Hasselblad H3DII-39 (Hasselblad USA, Inc., Parsippany, New Jersey, Figure 2(a)) camera obtaining natural colour imagery was employed in this study. It was equipped with a Kodak 39 megapixel (5412×7212 pixels) sensor measuring 36.8 by 49.1 mm, a 76.2 mm display for viewing imagery and the camera menu settings, a 35.8 mm focal length lens, and a rechargeable Li-ion battery (7.2 VDC/1850 mAh). Image capture rate of the camera is one image per 2 s. The images were stored on an external card with a storage capacity of 35 GB.

A global image locator (GIL, product number 3053300, Hasselblad USA, Inc., Parsippany, New Jersey, Figure 2) was attached to the camera. It is a global position receiver providing automatic creation and storage of GPS information for all H-system digital cameras (Hasselblad 2008). The GIL tags captured imagery with the following attributes: coordinated universal time (UTC time), longitude, latitude, altitude, and speed. The information is accessible with the Phocus software (version 2.5.2, Hasselblad, Sweden) accompanying the camera or other commercial software that is capable of retrieving the information. Additionally, a key-hole markup language (kml) file was created by the GIL, permitting the user to view the image acquisition location (latitude–longitude coordinates, World Geodetic System (WGS) 1984, datum) with Google Earth, other virtual globe programmes, and GIS software. It does not need an external power source and works seamlessly in the background for ease of use.



Legend

- Texas
- Presidio County
- Brewster County
- Rio Grande River
- Release Sites

Figure 1. Map of study area: (A) Contiguous USA showing the location of Texas, (B) Texas county map showing Presidio and Brewster counties and Rio Grande River, (C) close-up of Presidio and Brewster Counties showing the beginning (Candelaria, Texas) and ending (Lajitas, Texas) of the study transect, and (D) close-up showing beetle release sites (yellow circles). Starting with the first yellow circle close to Candelaria, the order of the release sites are as follows: Rancho Pensado I, Candelaria; Rancho Pensado II, Candelaria; Prieto Ranch, south of Candelaria; Ocotillo Springs; Burbach Property, Ruidosa; Farr Property, south of Ruidosa; Muniz Ranch, northwest of Presidio; Armendariz Ranch, northwest of Presidio; Gonzalez Ranch, northwest of Presidio; Alamito Creek Ranch, southeast of Presidio; West Entrance, Big Bend Ranch State Park; Redford, Big Bend Ranch State Park; Madera Canyon, Big Bend Ranch State Park; and Lajitas, Big Bend Ranch State Park.

Prior to each mission, the camera was focused by pointing it towards a target in the distance and turning the focusing ring until the target appeared in focus on the camera. The camera was placed in a camera mount and then the mount was positioned in a hole

Table 1. Name of saltcedar beetle release site, beetles released, and release date at 15 locations along the Rio Grande, in west Texas.

Location	Species	Release date
Rancho Pensado I, Candelaria	<i>Diorhadha sublineata</i>	2010
Rancho Pensado II, Candelaria	<i>D. elongate</i>	2007
Prieto Ranch, south of Candelaria	<i>D. elongate</i>	2007
Ocotillo Springs	<i>D. sublineata</i>	2009
Burbach Property, Ruidosa	<i>D. sublineata</i>	2009
Farr Property, south of Ruidosa	<i>D. sublineata</i>	2010
Muniz Ranch, northwest of Presidio	<i>D. sublineata</i>	2010
Armendariz Ranch, northwest of Presidio	<i>D. sublineata</i>	2010
Gonzalez Ranch, northwest of Presidio	<i>D. elongate</i>	2008
Alamito Creek Ranch, south east of Presidio	<i>D. sublineata</i>	2009
West Entrance, Big Bend Ranch State Park	<i>D. sublineata</i>	2010
Redford, Big Bend Ranch State Park	<i>D. sublineata</i>	2010
Portade, Big Bend Ranch State Park	<i>D. sublineata</i>	2010
Madera Canyon, Big Bend Ranch State Park	<i>D. sublineata</i>	2009
Lajitas, Big Bend Ranch State Park	<i>D. sublineata</i>	2009

within the belly of a Cessna 202 aircraft allowing the camera to view the surface below from a nadir position (Figure 2(B)). For each mission, the camera shutter was set at 1/500 of a second and the f -stop was $f/11$. During the missions, the imagery was manually captured by the operator by pressing a trigger tethered to the camera. The operator was able to view the ground below with a video camera (Figure 2(B)) that was mounted in the same frame as the digital camera and connected to a video monitor.

To provide a general understanding of changes occurring over time, imagery acquired from two separate dates will be discussed: 8 July 2011 and 8 September 2011. Images obtained on 8 July and 8 September were acquired at an altitude of 2500 and 3048 m above ground level resulting in a pixel resolution of approximately 0.5 and 0.6 m, respectively. Altitude differences were based on the airspace that the pilot was granted permission to fly into. The imagery for the July and September dates covered a 3.5 km by 2.7 km and 4.3 km by 3.2 km area, respectively. Imagery for both dates was required within 2 h of solar noon.

2.3. Image analysis

After each mission, the imagery was transferred from the camera storage card device to hard drive of a workstation for further processing. Analysis of the imagery was completed based on the following protocol: (1) opening the kml file to see the location of each image acquisition, (2) converting the imagery identified in the area of interest from its native format to a 16-bit tagged for information interchange format (tiff) file, (3) changing the tiff imagery to jpeg imagery and enhancing the latter, (4) viewing jpeg images to locate areas showing saltcedar damage, (5) labelling image showing damage in Google Earth, and (6) transferring Google Earth point file to geographic information software to produce a geographic database and to create a map showing where damage has occurred.

The imagery was acquired in the native format of the camera, 3FR raw (3FR raw is a proprietary image format created by Hasselblad digital cameras. It includes lossless compression reducing the required memory card space by 33%, and supports Hasselblads

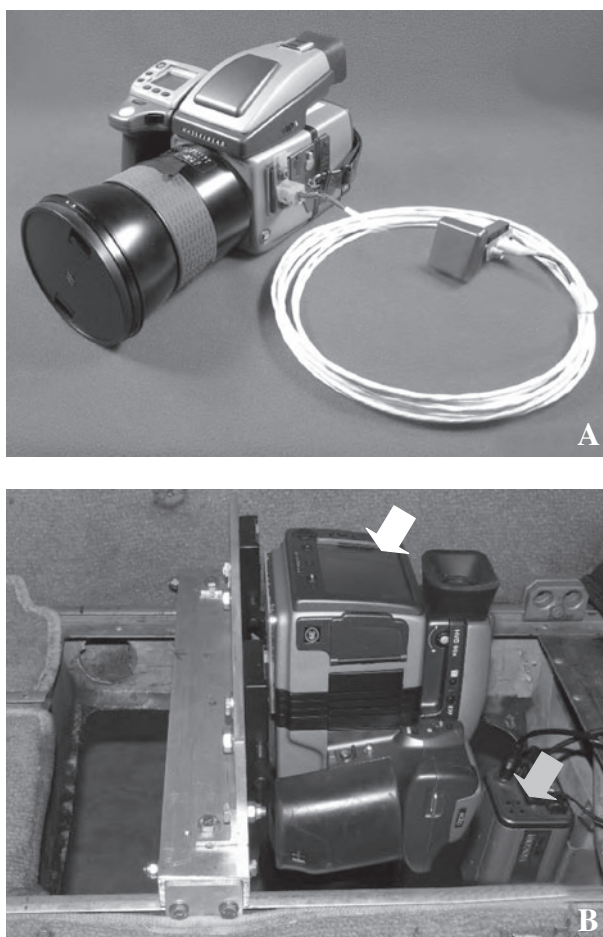


Figure 2. (A) Hasselblad camera (left) and global image locator (right). (B) Hasselblad camera (white arrow) and video camera (grey arrow) mounted in aircraft.

colour management solution.). The Phocus software was used to convert the 3FR raw files to 16 bit tiff files. The file size of the latter was 229 MB, requiring excessive random access memory to view the files.

Irfanview (version 4.28, Vienna University of Technology) is a small compact graphic viewer that lets the user view various types of imagery and video; it also has batch capabilities, allowing the analyst to perform a multitude of tasks during batch processing. The batch mode was used to rotate imagery if needed, auto-adjust the colours (fine-tuned the colours by automatically adjusting gamma and brightness values), and save the files in jpeg format [save quality 50 (compression rate) and file size 10 MB]. Files with that quality and size maintained the integrity needed for qualitatively assessing the imagery and viewing without affecting the memory of the computer during the process. Evaluation of the 2011 imagery indicated that the best stage to detect the beetle damage qualitatively was when the foliage was showing severe stress related to the beetle and larvae feeding and when the plants were totally defoliated (Figure 3).

Image interpretation required viewing the jpeg image and the GIL kml file for each date. The kml file was viewed in Google Earth, providing the background imagery



Figure 3. Ground level images of (A) healthy saltcedar tree foliage-closeup image of canopy, (B) intermediate symptoms of beetle and larvae feeding to saltcedar tree canopy-closeup image of canopy, (C) severe symptoms of beetle and larvae feeding to a saltcedar tree canopy-closeup image of canopy photo, and (D) total defoliation of saltcedar tree canopies caused by beetle and larvae feeding.

needed to help the analyst understand the orientation of the jpeg image. The jpeg image was zoomed into to search for trees damaged by the beetle and larvae. A 60% overlap occurred between images; therefore, every third image was appropriate for the analysis. The Irfanview software was used to survey the imagery.

The GIL malfunctioned on 8 September 2011; therefore, it did not record the coordinate system information. The latitude–longitude coordinates were entered manually into Google Earth. Images overlapping the location of the 8 July 2011 images were selected for 8 September, permitting adequate comparison of the imagery between the two dates.

For display purposes and to show basic changes over time, three study sites are discussed (Figure 4): Rancho Pensado II (30° 7.647'N, 104° 40.672'W), Alamito Creek Ranch (29° 31.208'N, 104° 17.261'W), and Portade (29° 22.694'N, 104° 7.269'W, image is approximately 2.4 km northwest of release site).

Beginning in 2008, beetle releases and movements in the researched area have been monitored by Sul Ross University personnel. Monitoring includes conducting field surveys to confirm the presence of saltcedar leaf beetles and larvae (counts of beetles and larvae) at release sites (Table 1), to determine damage caused by the beetles and larvae feeding (drive-by-surveys), and to provide general information pertaining to beetle movement (Ritzi & Hilscher 2011). Their reports and reports by federal government personnel have been posted to a secure website. Based on these reports, damages to the saltcedar trees were caused by saltcedar leaf beetles and larvae. In addition, damage not

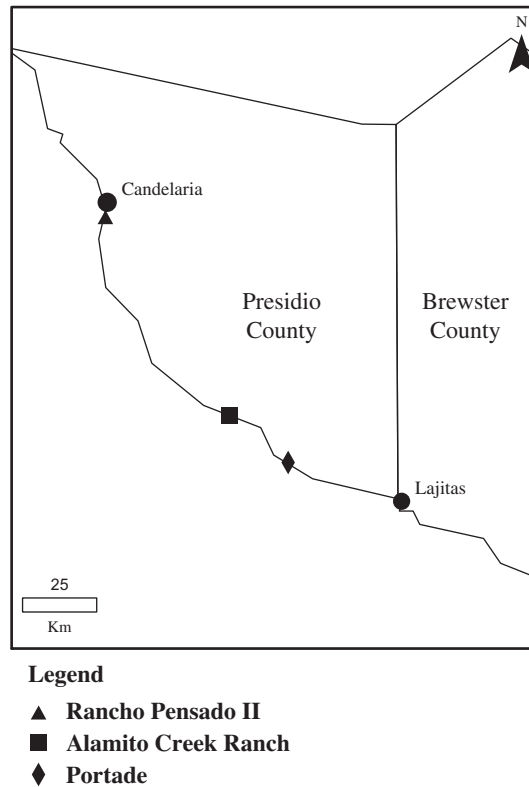


Figure 4. Location of study sites used to show changes overtime in saltcedar canopies affected by saltcedar leaf beetle and larvae feeding.

caused by beetle and larvae feeding were included in the reports on the website (Ritzi & Hilscher 2011). Note: The surveys conducted by Sul Ross University personnel were divided into two subsets: (1) Lajitas, Texas, to Presidio, Texas and (2) Presidio, Texas, to Candelaria, Texas (Figure 1(C)). The subsets were not monitored in the same week; surveys were conducted per subset on alternate weeks every two weeks. For the 2011 calendar year, surveys began on 14 January 2011 and ended on 16 December 2011 (Ritzi & Hilscher 2011). Surveys within two weeks of the image acquisition dates were used to help in image interpretation. The author also conducted drive by surveys along the transect to confirm damage to saltcedar trees and also navigated as close as possible to the centre coordinates of selected aerial images to document damages to the saltcedar trees. A hand-held GPS unit was used for navigation. Surveys were conducted on 19–20 July 2011 for the July imagery and on 5–6 October 2011 for the September imagery.

The GIS database was developed by importing the kml coordinate file information to ArcMap10 (ESRI 2011, Release 10, Redlands, California). Vector data as shape-files containing county boundaries and the Rio Grande River were downloaded from ArcGIS online (Using a direct link between ArcMap10 and ArcGIS online to complete download) and the Texas Water Development Board (<http://www.twdb.state.tx.us/mapping/gisdata.asp>) websites, respectively. Coordinates for cities listed on the GIS maps were determined with Google Earth; this information was converted to shape-files using ArcMap10. Data layers obtained from the various sources had its own coordinate

system and datum. For the GIS maps, all layers were converted into the latitude–longitude coordinate system and the WGS 1984 datum. The coordinates of the images were overlaid onto the other layers for display purposes. Also, the imagery was linked to its corresponding point on the map, allowing the user to view the imagery related to a specific point.

3. Results and discussion

3.1. *Qualitative assessment of the imagery*

Saltcedar trees exhibiting severe feeding damage (Figure 3) and those that were totally defoliated (Figure 3) were readily identifiable in the imagery. The former appeared in orange to brown colour tones and the latter exhibited grey colour tones. These two stages were used to pinpoint saltcedar canopies affected by beetle and larvae feeding.

Example images of locations showing feeding damage to saltcedar trees for 8 July 2011 and 8 September 2011 are presented in Figures 5–7. For the Portade Big Bend Ranch State Park study area, the damage transitioned from severe (orange foliage in saltcedar trees) to totally defoliated (grey colour on imagery) between the two dates (Figure 5). At the Alamito Creek Ranch study site, saltcedar trees exhibited severe feeding damage along with total defoliation (Figure 6). Saltcedar trees had a similar appearance in the imagery for 8 September 2011 (Figure 6). Differences between damaged saltcedar trees and other green vegetation were apparent on the imagery. At the Rancho Pensado II, Candelaria site, few saltcedar trees exhibited severe damage (Figure 7). By 8 September 2011, saltcedar trees exhibiting severe feeding damage were readily distinguished in the imagery. The colour of saltcedar tree canopies changed from green to orange brown in the imagery (Figure 7(C) and (D)).

Beetles and larvae feed on foliage of saltcedar trees, reducing its ability to complete photosynthesis, thus decreasing the amount of starches and sugars produced by the plant. As chlorophyll deteriorates, its production is decreased, and other pigments that were masked by the presence of chlorophyll are now more actively involved in reflecting visible light, resulting in an increase of green and red light reflectance by stressed trees. The increase in visible light reflectance causes the stressed saltcedar trees to appear in the orange colour as seen in the imagery (Figures 5–7). Totally defoliated trees consist of stems and branches appearing in a dark grey colour. Stems and branches reflect blue, green, and red light equivalently, causing the greyish colour seen in the imagery (Figures 5 and 6).

3.2. *Geographic information database*

Distribution maps displaying the location of damaged saltcedar trees along the 155.8 km transect are shown in Figures 8 and 9. Severe damage and defoliation were evident on all of the images shown on the maps; nevertheless on 8 July 2011, the damage and defoliation were more prominent between Lajitas and Ruidosa (Figure 8(A)). By 8 September 2011, the damage northwest of Ruidosa was becoming more evident (Figure 9), as shown in Figure 7 (acquired northwest of Ruidosa).

GISs also have unique tools the analyst can employ for decision support. Figure 8 (B) shows the centre coordinate of the imagery in relation to the beetle release site at Alamito Creek and examples of how the analyst could determine imagery obtained within 5 km of the release site based on the centre coordinates of each image. Figure 10



Figure 5. Aerial imagery of a subsection of the Portade Big Bend Ranch State Park site: (A) 8 July 2011 (0.50 m pixel resolution) and (B) 8 September 2011 (0.60 m pixel resolution). Arrows point to saltcedar trees exhibiting damage caused by the biological control agent-saltcedar leaf beetle. Close-up of section pointed to by yellow arrow on the right of both images: (C) 8 July 2011-within dashed yellow box, yellow arrow points to damaged saltcedar trees appearing in orange brown colour tones and (D) 8 September 2011-within dashed yellow box, yellow arrow points to damaged saltcedar appearing in mixture of grey colour tones. Scale 5A–5B: 1 cm \approx 0.22 km; Scale 5C–5D: 0.5 cm \approx 0.03 km.

presents layers used to create the map (solid line box), information pertaining to a specific point on the map (square dot box), the location of the image on the map, and the image linked to the point (long dash box).

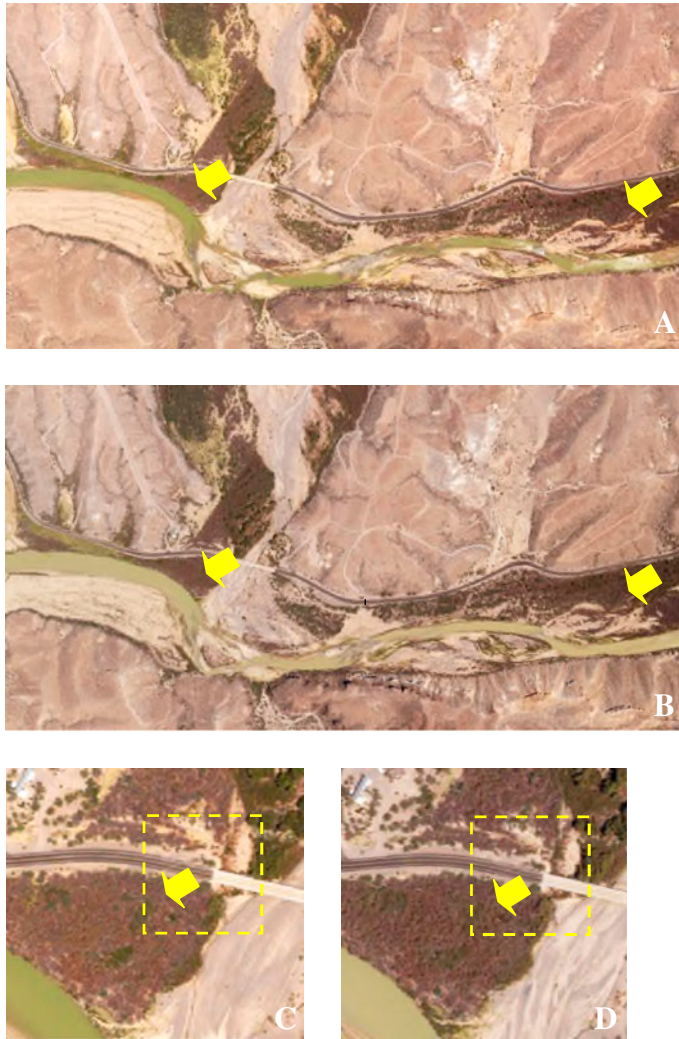


Figure 6. Aerial imagery of a subsection of the Alamito Creek Ranch: (A) 8 July 2011 (0.50 m pixel resolution) and (B) 8 September 2011 (0.60 m pixel resolution). Arrows point to saltcedar trees exhibiting damage caused by the biological control agent-saltcedar leaf beetle. Close-up of section pointed to by left yellow arrow on (A) and (B): (C) 8 July 2011 and (D) 8 September 2011; within dashed yellow box for C and D, yellow arrow points to damaged saltcedar appearing in mixtures of orange, brown, and grey colour tones. Scale 5A–5B: 1 cm \approx 0.16 km; Scale 5C–5D: 0.5 cm \approx 0.03 km.

3.3. Perspectives of the study

The results concurred with others that have used aerial imagery, GPS, and GIS to derive point distribution maps showing locations of invasive plant infestations (Everitt et al. 1994, 1996, 1999, 2003, 2006). Findings of this study have a unique agreement with that of Everitt et al. (2006). They indicated that the best time to separate saltcedar from other cover types was when it turned orange during senescence, which occurs in early December. When the saltcedar leaf beetle and larvae feed on saltcedar trees, the plant's canopy changes to an orange or orange brown colour leading to it being readily



Figure 7. Aerial imagery of a subsection of the Rancho Pensado II, Candelaria release site: (A) 8 July 2011 (0.50 m pixel resolution) and (B) 8 September 2011 (0.60 m pixel resolution). Yellow arrows point to saltcedar trees exhibiting damage caused by the biological control agent-saltcedar leaf beetle. Cyan arrow points to saltcedar trees not showing severe feeding damage in the imagery. Close-up of section pointed to by the cyan and yellow arrows on the right of figures (A) and (B), respectively: (C) 8 July 2011-within dashed yellow box, yellow arrow points to saltcedar tree canopies with green colour tone and (D) 8 September 2011-within dashed yellow box, yellow arrow points to damaged saltcedar canopies appearing in orange brown colour tones. Scale 5A–5B: 1 cm \approx 0.24 km; Scale 5C–5D: 0.5 cm \approx 0.04 km.

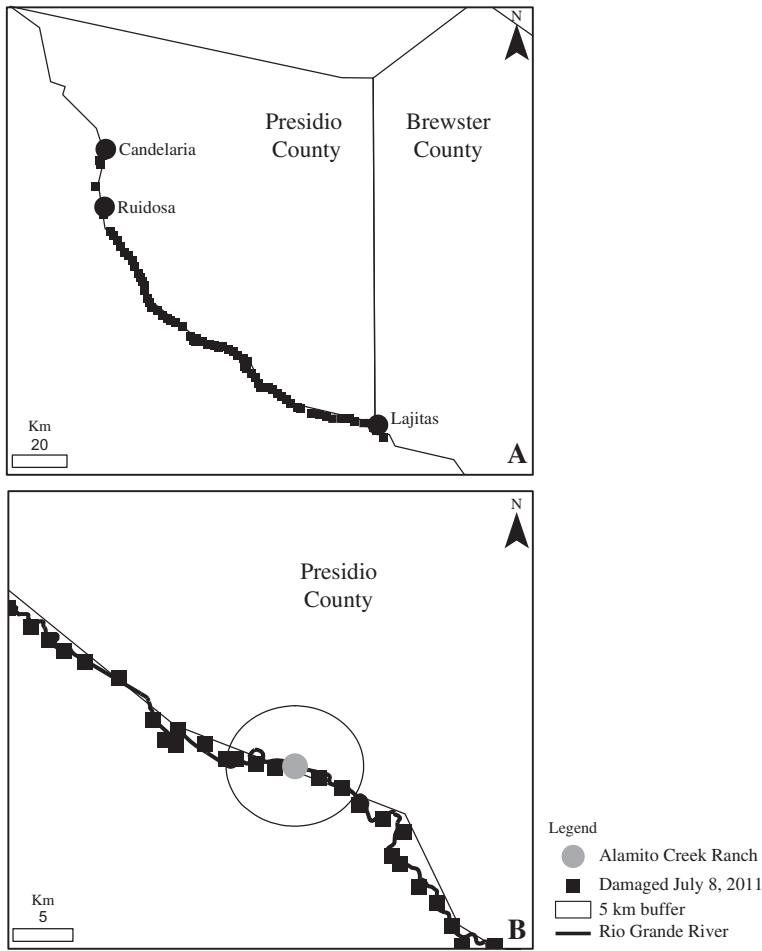
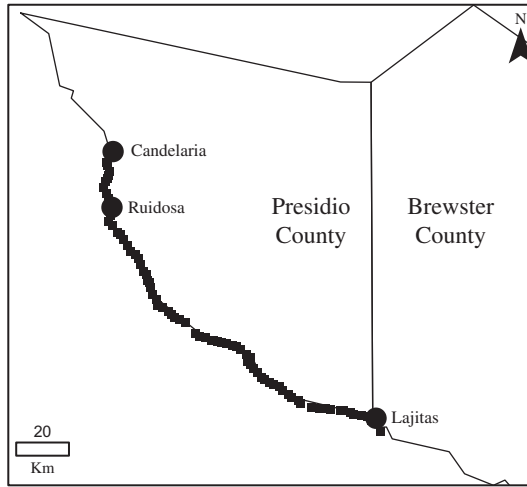


Figure 8. (A) Distribution map of feeding damage areas on 8 July 2011 and (B) close-up showing application of the GIS to create a buffer enclosing the centre coordinates of imagery within five kilometres of the Alamito Creek Ranch release site.

separated from other green vegetation in the imagery. Also, the results showed that imagery collected every two months was appropriate for monitoring biological control of saltcedar in west Texas.

Others have evaluated and demonstrated applications of satellite systems to monitor biological control of saltcedar. Vegetation indices derived with red and near-infrared bands of coarse resolution satellites such as LANDSAT TM (Archambault et al. 2009), ASTER (Dennison et al. 2009), and MODIS (Dennison et al. 2009) have shown good potential for monitoring chemical and biological defoliation of saltcedar. The coarse spatial resolutions of those satellites limit their application to dense stands of saltcedar. For aircraft, the elevation above ground level is adjustable, allowing the user to select the appropriate altitude to improve the spatial resolution and to complete the mission.

In addition, medium to high format digital camera systems are becoming common place systems to use in aircraft imaging. Up to this point no research has been conducted in which a digital camera system has been integrated with GPS and GIS



Legend

- Damaged September 8, 2011

Figure 9. (A) Distribution map of feeding damage areas on 8 September 2011.

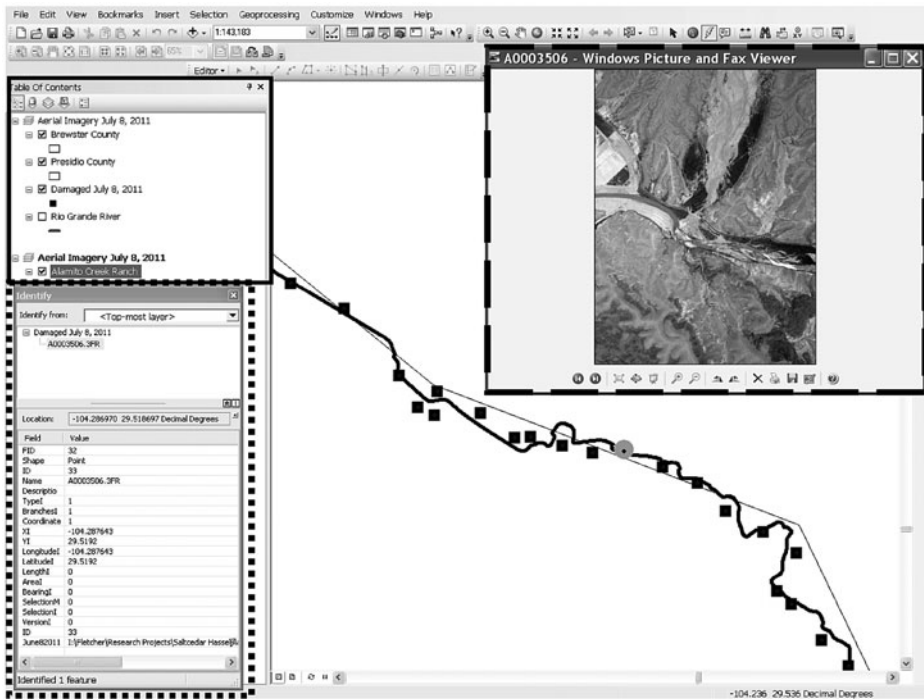


Figure 10. Example of information stored in the GIS. Solid line box represents layers used to create the map, square dot box shows information related to an image acquired by the camera-black squares on the map located at the right, and long dash box corresponds to the image that is linked to that point.

Downloaded by [] at 06:57 23 March 2015

technologies to monitor biological control of saltcedar. The strong suit of the imagery is that it is in digital format and immediately viewable after image acquisition. The kml file created by the GIL attached to the camera was useful for identifying the location of the imagery in digital globes, such as Google Earth, which was employed in this study. Furthermore, the GPS information can easily be plotted on river, county, and state digitised GIS maps to derive maps of affected locations. The GIS can also serve as a database for archived imagery. Additionally, the system can be placed in any aircraft that has a hole in the belly, thus, increasing the application of the system to monitor biological control of saltcedar.

Disadvantages of using the airborne imagery as described in this study are as follows. It is not georeferenced; therefore, the imagery cannot be used as a backdrop for other layers. Also, only approximate measurement damage is extractable from the imagery.

4. Conclusions

This study demonstrated that remote sensing integrated with GPS and GIS technologies has high potential as a tool for monitoring biological control of saltcedar in west Texas. In natural colour imagery, plants exhibiting severe feeding damage and total defoliation caused by beetle and larvae feeding appeared in orange to orange brown colour tones and grey colour tones, respectively. By linking the camera system with GPS, the location of the centre coordinate for each image was recorded, allowing the viewer to plot the location of the imagery in a GIS as well as digital globes such as Google Earth. It is believed that imagery acquired every two months with this system should suffice for monitoring biological control of saltcedar in west Texas. Based on field reports posted by state and federal officials, it is postulated that image collection should begin in May followed by data collection every other month. The results of this study show a practical method to use for monitoring biological control of saltcedar. Saltcedar plants stress symptoms are the same when it comes to beetle feeding, thus, this technique is applicable to other areas.

Acknowledgements

The author thanks Dr Jack DeLoach, Dr Chris Ritzi, Juan Ramos, Isabel Cavazos, Fred Gomez, Michael Ohlinger, James Tracy, Ann Marie Hilshcer, and Jim Forward for their assistance in this study.

References

- Archambault V, Auch J, Landy J, Rudy G, Seifert C. 2009. Utilizing remote sensing to supplement ground monitoring of *Diorhabda elongata* as control agent for *Tamarix ramosissima* in Dinosaur National Monument. In Proceedings of American Society of Photogrammetry and Remote Sensing, Annual Conference; 2009 March 9–13; Baltimore, Maryland.
- Baker HG. 1974. The evolution of weeds. *Annu Rev Ecol Syst.* 5:1–24.
- Baum BR. 1967. Introduced and naturalized tamarisks in the United States and Canada (*Tamaricaceae*). *Baileya.* 15:19–25.
- Brotherson JD, Winkel Von. 1986. Habitat relationships of saltcedar (*Tamarix ramosissima*) in central Utah. *Great Basin Naturalist.* 46:535–541.
- Crins WL. 1989. The Tamaricaceae in the southeastern United States. *J Arnold Arbor.* 70: 403–425.

- DeLoach CJ, Carruthers RI, Lovich JE, Dudley TL, Smith SD. 2000. Ecological interactions in the biological control of saltcedar (*Tamarix* spp.) in the United States: toward a new understanding. In: Delfosse ES, editor. Proceedings of the Tenth International Symposium on Biological of Weeds; 1999 Jul 4–9; Bozeman, MT, USA.
- Dennison PE, Nagler PL, Hultine KR, Glenn EP, Ehleringer JR. 2009. Remote monitoring of tamarisk defoliation and evapotranspiration following saltcedar leaf beetle attack. *Remote Sens Environ.* 113:1462–1472.
- DiTomaso JM. 1998. Impact, biology, and ecology of saltcedar (*Tamarix* spp.) in the Southwestern United States. *Weed Technol.* 12:326–336.
- ESRI. 2011. ArcGIS Desktop: Release 10. Redlands (CA): Environmental Systems Research Institute.
- Everitt JH, Anderson GL, Escobar DE, Davis MR, Spencer NR, Andrascik RJ. 1994. Light reflectance and remote sensing of Big Bend loco (*Astragalus mollissimus* var. *earlei*) and wooton loco (*Astragalus wootonii*). *Weed Sci.* 42:115–122.
- Everitt JH, Escobar DE, Alaniz MA, Davis MR. 1996. Using spatial information technologies to map Chinese tamarisk (*Tamarix chinensis*) infestations. *Weed Sci.* 44:194–201.
- Everitt JH, Yang C, Escobar DE, Webster CF, Lonard RI, Davis MR. 1999. Using remote sensing and spatial information technologies to detect and map two aquatic macrophytes. *J Aquat Plant Manage.* 37:71–80.
- Everitt JH, Alaniz MA, Davis MR. 2003. Using spatial information technologies to detect and map waterhyacinth and hydrilla infestations in the Lower Rio Grande. *J Aquat Plant Manage.* 41:93–98.
- Everitt JH, Yang C, Davis MR. 2006. Remote mapping of saltcedar in the Rio Grande System of Texas. *Tex J Sci.* 58:13–22.
- Everitt JH, Yang C, Fletcher RS, Deloach CJ, Davis MR. 2007. Using remote sensing to assess biological control of saltcedar. *Southwestern Entomol.* 32:93–103.
- Gaskin JF, Schaal BA. 2002. Hybrid *Tamarix* widespread in US invasion and undetected in native Asian range. *Proc Nat Acad Sci.* 99:11256–11259.
- Gaskin JF, Schaal BA. 2003. Molecular phylogenetic investigation of US invasive *Tamarix*. *Syst Bot.* 28:86–95.
- Hasselblad. 2008. Global image locator. Gothenburg: Hasselblad.
- Nagihara S, Hart CR. 2007. Use of satellite remote sensing in monitoring saltcedar control along the Lower Pecos River, USA. Texas Agricultural Experiment Station, TR-306.
- Ritzi CM, Hilscher AM. 2011. Saltcedar beetle project [Online]. [cited 2011 Dec 12]. Available from: <http://www.sulross.edu/scbp/>
- USDA. 2005. Program for biological control of saltcedar (*Tamarix* spp.) in thirteen states. United States Department of Agriculture-Animal and Plant Health Inspection Service.